



**HAL**  
open science

# Numerical investigation of the surface effects on the dwell time during the sweeping of lightning arcs

L. Tholin, P. Chemartin, F. Lalande

► **To cite this version:**

L. Tholin, P. Chemartin, F. Lalande. Numerical investigation of the surface effects on the dwell time during the sweeping of lightning arcs. 2013 International Conference on Lightning and Static Electricity (ICOLSE 2013), Sep 2013, SEATTLE, United States. hal-01068639

**HAL Id: hal-01068639**

**<https://onera.hal.science/hal-01068639>**

Submitted on 26 Sep 2014

**HAL** is a multi-disciplinary open access archive for the deposit and dissemination of scientific research documents, whether they are published or not. The documents may come from teaching and research institutions in France or abroad, or from public or private research centers.

L'archive ouverte pluridisciplinaire **HAL**, est destinée au dépôt et à la diffusion de documents scientifiques de niveau recherche, publiés ou non, émanant des établissements d'enseignement et de recherche français ou étrangers, des laboratoires publics ou privés.

# NUMERICAL INVESTIGATION OF THE SURFACE EFFECTS ON THE DWELL TIME DURING THE SWEEPING OF LIGHTNING ARCS.

Tholin<sup>1</sup>, L. Chemartin<sup>1</sup>, P. Lalande<sup>1</sup>F.

<sup>1</sup> Onera - the French Aerospace Lab  
Châtillon (F-92322), France

[laurent.chemartin@onera.fr](mailto:laurent.chemartin@onera.fr), [fabien.tholin@onera.fr](mailto:fabien.tholin@onera.fr), [lalande.philippe@onera.fr](mailto:lalande.philippe@onera.fr)

## ABSTRACT

During a lightning strike in flight, the arc sweeps back along the aircraft surface by jump under the effects of the aerodynamic flow. This mechanism is called swept stroke. The dwell times at each attachment point vary according to the nature of the surface; the local geometry and air flow; and the current waveform which could cause reattachment if a current peak occurs.

This paper is focused on the effects of the surface on the dwell time value. The parameters studied are the thickness of the boundary layer, and the presence of insulating coatings on the surface. 3D Numerical simulations of DC arcs along planar surfaces in the presence of a flow are carried out based on the Magneto Hydrodynamic (MHD) approach. The dynamics and the arcs instabilities are investigated with a special attention to the expansion radius, the tortuosity, and the internal voltage gradient. The effects of the boundary layer thickness and the presence of insulating layers on the dwell-time are discussed and the criteria for reattachment are examined. Finally, an example of dwell-time estimation is considered and the effects of electric and thermal constraints are discussed.

## INTRODUCTION

During a lightning strike in flight, the lightning arc may break through the insulating layers covering the aircraft skin, such as paint or alumina layers. Then, an electric contact between the lightning arc and the conductive aluminum skin is obtained and the continuing current phase of the lightning flash may start, with DC currents of hundreds of Amps [1]. Due to the aircraft displacement, the arc is stretch to maintain the electric contact between the lightning arc, immobile relatively to the air, and the conductive aluminium skin (see figure 1 t1-t2). Because the length of the arc increases quickly, the plasma resistance increases as well. As a result, to maintain the DC current, the potential

drop in the plasma column has to increase at the same rate. Due to the stretching of the arc parallel to the aircraft body, the distance between the electric arc column and the skin of the aircraft may become very small, of the order of the boundary layer thickness  $\delta$  (see figure 1 t3). This configuration makes possible important thermal constraints and important electric-fields between the arc column and the conductive skin. If strong enough, the breakdown of the resistive layers under electrical and thermal constraints generates a new connection between the electric arc and the conductive layer farther on the aircraft. The current then flows through this new path to the skin, and the old arc channel gets colder and extinguish (figure 1 t4).

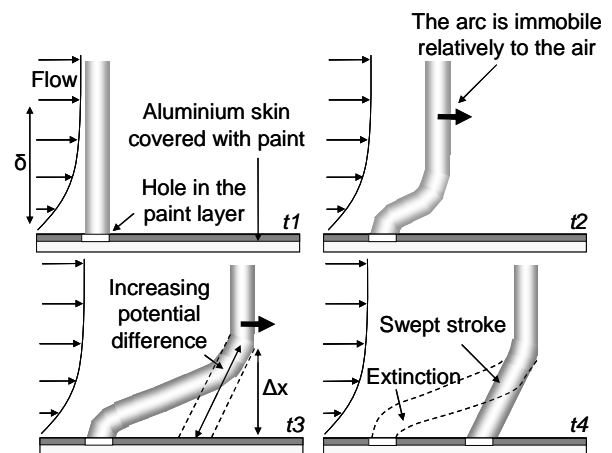


**Figure 1:** Swept stroke reattachment process in the frame of reference of the plane: (t1) A lightning arc attaches on the skin of a plane: the DC current has to pass through a hole in the insulating layers. (t2) the lightning arc column is convected by the relative wind which has a boundary layer velocity profile of thickness  $\delta$ . (t3) The potential difference increases between the arc column and the skin. (t4) Breakdown occurs, a new electric contact in the resistive layer appears and a new current path is created.

This reattachment phenomenon of lightning arcs called “swept stroke”, may start again several times

during the sweeping phase with a characteristic time for reattachment referred as “dwell time” [1]. The dwell-time is of considerable importance to predict the lightning arc trajectories on an aircraft body, and particularly the residence time of the arc root to some specific regions such as fuel tank area [2]. Moreover, as explained in [1], many different techniques have been studied in order to prevent the damages to the aircraft skin such as coatings, thicker aluminium skins, titanium skins, meshes, or projection techniques, but a better fundamental understanding of the sweeping phenomenon is necessary for further improvements. The strategy in this work is to perform numerical simulations of a sweeping arc and to focus on the evolution of the maximum potential difference across the insulating layers as the arc column is stretch over long distances. Whatever the insulating layers thickness, the maximum difference in electric potential corresponds always to the place of maximum potential at the outer surface of the aircraft skin, since the potential drop in the aluminium skin and the arc column arc are negligible due to their higher conductivities. The evolution of this maximum surface potential is non intuitive since the arc, far from being straight, may present a high tortuosity due to the complex MHD instabilities in the boundary layer.

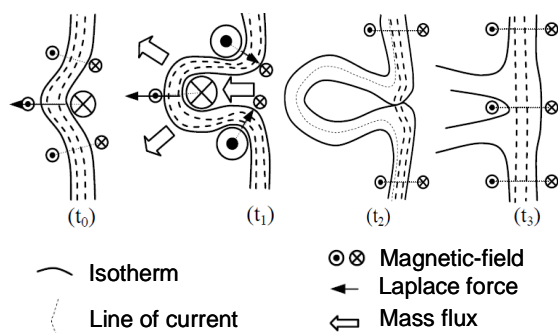


**Figure 2 :** MHD instability in an arc column: ( $t_0$ - $t_1$ ) A loop of current is growing under the effect of its own magnetic pressure (Lorentz self-force). ( $t_2$ ) The loop is closed and the current can follow a straight path. ( $t_3$ ) the loop gets colder due to thermal dissipation processes and finally disappears in the absence of Joule heating.

One of the main MHD instability mechanism consists in the formation of current loops expanding in radius due to their own Lorentz self-forces [3]. Such loops may grow in radius and eventually disappear through reconnection processes as explained on figure 2. Moreover, the structure of the arc may also be influenced by the aerodynamic flow, and the thermal and electrical properties of the aircraft skin. As a consequence, many different parameters may have a significant influence on the arc dynamics: The thickness of the insulating layers, their permittivity and dielectric strength, the velocity of the airplane, the boundary layer thickness, and velocity profile (laminar or turbulent), and the current in the lightning arc.

### MHD Model for the lightning arc

The most accurate way to simulate the sweeping phase of a lightning arc is the magneto-hydrodynamic (MHD) approach. Indeed, the interaction between the magnetic field and the fluid plays a crucial role for the dynamics of lightning, even more notably during the sweeping of a lightning arc along an aircraft surface. In the vicinity of the boundary layer, the aerodynamic flow is very likely to bend and stretch the lightning arc. The convection of the conductive air plasma may induce Lorentz induction effects and the Laplace forces may accelerate or deflect the airflow. The MHD approach, widely used in the modeling of electric arcs such as unsteady DC electric arcs [4], switching arcs and circuit breakers [5], is able to catch this complex interaction by solving the fully coupled Navier-Stokes equations and the Maxwell equations in the limit of the MHD approximation (hypothesis of plasma quasi-neutrality and negligible displacement current over time). The plasma is assumed to be at LTE (Local Thermodynamic Equilibrium) for the whole calculations performed in this work. The physical properties ( $C_p$ ,  $\lambda$ ,  $\sigma$  ...) and the chemical composition under LTE assumption are entirely determined by the temperature and the pressure of the plasma.

In this work, tabulated values based on the work of D'Angola et al. [6] are used. The plasma properties range from 50 to 60 000 K for temperature, and from 0.01 to 100 atm for pressure. Such very high pressure shockwave formation may be obtained on short timescales during the first stages of a lightning stroke. However, during the sweeping phase with DC current, it is reasonable to assume that transient compressible flow phenomena, such as pressure waves, have a small influence on the arc dynamics: The characteristic evolution timescales of a lightning arc during the sweeping phase is larger (ms) than the characteristic acoustic timescales for pressure equilibrium in the plasma (10  $\mu$ s). Then, it is assumed an expandable flow in a first approximation, which means that the acoustic waves travel at infinite speed making the total pressure constant in the whole computational domain. Then, the regions heated by the lightning arc are instantaneously in pressure equilibrium with the surrounding air due to a lower density and static pressure variations always result from velocity variations. The resolution of the 3D MHD equations has been performed with *Code Saturne*, the EDF's general computational fluid dynamics software based on a co-located finite volume method [7]. *Code Saturne* is well adapted to solve expandable flows with heat transfer and it includes a standard electric arc model able to solve the Maxwell equations in the static approximation (negligible displacement current and self-induction). The simulation domain (see figure 3) is a rectangular box with a length of 120 cm (x direction), a 20 cm width (y direction) and a 10 cm height (z direction).

The time-step used in this work to catch properly the arc dynamics during the sweeping phenomena is 1  $\mu$ s. For such timescales, electromagnetic waves propagate on distances much larger than the simulation domain (300 m) and the static approximation is very well adapted. The Maxwell-Ampere's equation and the conservation equation of the current with displacement current neglected can be written in the form of system [8].

$$(1) \quad \begin{aligned} \vec{\nabla} \times \vec{B} &= -\Delta \vec{A} = \mu_0 \vec{J} \\ \vec{\nabla} \cdot \vec{J} &= -\vec{\nabla} \cdot \sigma \vec{\nabla} \phi = 0 \end{aligned}$$

The vector potential A and the electric potential  $\phi$  are computed in *Code Saturne* by solving this system of Poisson's equation. More details about the numerical methods used in *Code Saturne* to model the dynamics of the arc can be found in [4], [7] and [8]. In order to study the sweeping phase on a aircraft body during a few ms, a simplified geometry is considered: The skin of the aircraft is modeled by a 2 mm thick planar sheet of aluminum (plane xy on figure 3). The skin may be covered by a thin layer of alumina (10  $\mu$ m) and a layer of aeronautic paint (100-200  $\mu$ m). Both the alumina and the paint layers are highly resistive materials, and the lightning arc has to break through these layers so that the current can reach the underneath conductive aluminum skin. The modeling of the destruction of the insulating layers by thermal, mechanical, and electrical constraints is a very complex challenge beyond the scope of this study. Then in this work, we do not model the breakdown of the insulating layers, and two different situations have been considered.

	<i>Inlet</i>		<i>Outlet</i>		<i>Lateral</i>		<i>Top</i>		<i>Bottom</i>
	Metal	Air	Metal	Air	Metal	Air	Plasma	Air	Metal
$\phi$	0	N	0	N	0	N	U	N	N
Ax	0		0		0		0		0
Ay	0		0		0		0		0
Az	0		0		0		N		0
P	isolib		isolib		isolib		isolib		isolib
Vx	Vbl	Vp	isolib		Vp	Vbl	isolib		isolib
Vy	0		isolib		0		isolib		isolib
Vz	0		isolib		0		isolib		isolib
H	href		href		href		N		isolib

**Table 1** : Boundary conditions: N: Neumann boundary condition with zero gradient ; isolib : free outlet boundary condition implemented in *Code Saturne* ; Vp : Velocity of the plane (200 m/s) ; Vbl : Boundary layer velocity calculated analytically (Blasius velocity profile for laminar flow) ; href : reference enthalpy for the air.

In the first one, the presence of an insulating layer is neglected. The arc root moves freely without the effect of the insulating layers (zero surface resistivity). Details about the simulation of this first case can be found in [8]. In the second case, we consider the opposite situation with the presence of ideal dielectric paint and alumina layers, of infinite surface resistivity, and infinite dielectric strength. For that case, we assume as initial condition a circular hole in the paint and the alumina of 5 mm radius. It is representative of the damage that would be produced by the initial high current stroke that occurs on very short timescales before the continuing current phase. Consistently, an arc column in the  $z$  direction of 5 mm radius is placed above the hole in the air (see figure 1). The temperature profile in the arc column is Gaussian with a maximum at the center of 10 000K, and a corresponding conductivity of  $0.38 \times 10^4$  S/m [6]. The current in the lightning arc is set to 400 A in all the simulations. To maintain the current constant, a Dirichlet boundary condition on the electric-potential  $\varphi$  is applied at the Top boundary (see table 1 and figure 1).

The imposed voltage value is computed at each time-step explicitly with the plasma resistance evaluated at the previous time-step to maintain a constant current in the arc column as performed in [8]. We have considered an airplane flying at a velocity  $V_p = 200$  m/s. The simulations are performed in the aircraft frame of reference: the skin of the aircraft is immobile in the computational domain but the flow outside of the boundary layer has a velocity equal to  $V_p$  in the  $x$  direction. In the boundary layer, a laminar velocity profile computed thanks to the Blasius equation is imposed on the boundaries at every timestep and in the all computational domain at  $t=0$  s for initialization. Because the flow is from left to right ( $+x$ ), the right boundary condition is an outlet boundary condition instead. Table 1 summarizes the boundary conditions used in this work for the different variables solved in *Code Saturne* in the frame of reference of the aircraft.

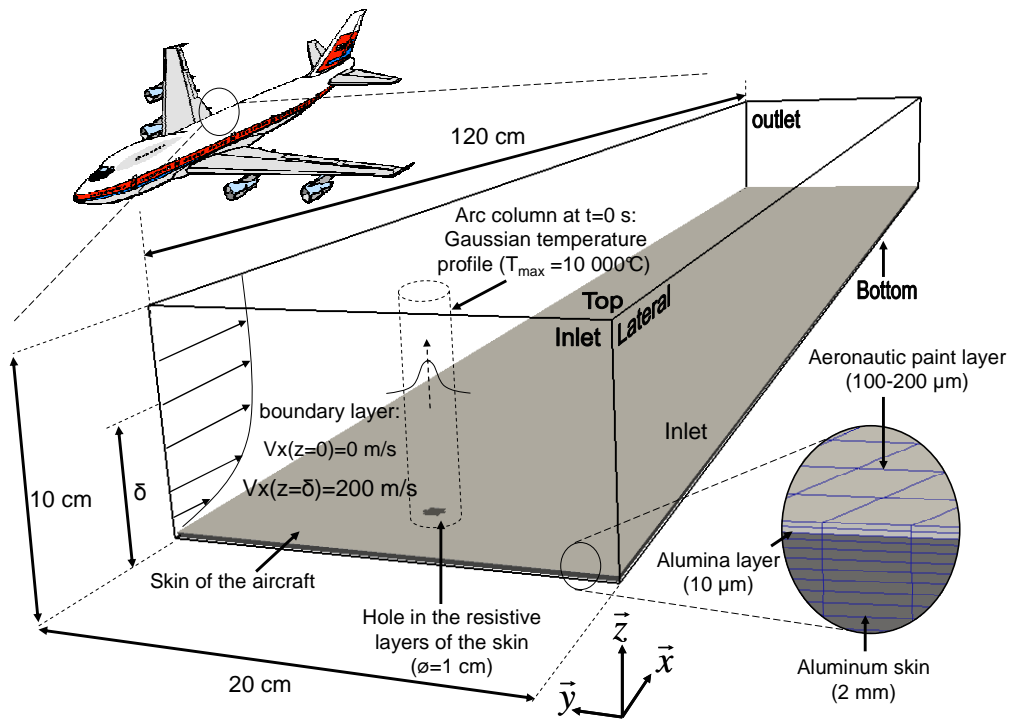


**Figure 3:** Schematic view of the simulation domain in the frame of reference of the plane: the skin of the plane is not moving but the velocity outside of the boundary layer is equal to the plane velocity  $V_p$ .

## Numerical Results

The first situation consists in the simulation of an arc column of 400 A over a 2 mm thick uncovered aluminium skin. For computational cost reasons, it has been performed in the atmospheric frame of reference contrary to the situation depicts on figure 3 (air is immobile outside of the boundary layer and the skin of the plane is moving). In this simulation, the boundary layer thickness is  $\delta=10$  mm and the velocity of the plane is 100 m/s. Because the lightning arc is directly connected to the aluminium skin, the dwell-time is in this case quite short, in the range 500  $\mu$ s – 3 ms, which is coherent with the values given in [1]. For this particular case it was then possible to simulate up to fifty reattachments [8]. Figure 4 shows a sliced view of the temperature and the electric-field just before one of these reattachments. The cutting plane is the plane  $y=0$  (see figure 3), and the isosurface  $T=8000$  K is also shown in 3D by transparency of the cutting plane. It can be seen clearly that just before reattachment the electric-field reaches a maximum very close to the surface of the skin (white arrow). The following reattachment takes place at this precise location, taking advantage of a high electric-field, a large temperature gradient and a small distance between the arc column and the skin. The atmospheric frame of reference facilitates a lot the simulations in the case of small dwell-times since the computational domain may be much smaller than the total distance traveled by the arc on the surface. However, in the case of a skin covered with insulating layers, the dwell-time may be much larger and the numerical simulation of the reattachment is then computationally expensive since the lengths of the arc and the numerical domain have also to be much larger in this case. This issue limits the purpose of simulations in the atmospheric frame of reference. Moreover, in this frame of reference, it is not possible to simulate more realistic shapes, such as wings, antennas, or fuel tank assemblies. Then, for the second situation with insulating dielectric layers, simulations are carried out in the aircraft frame of reference (figure 3). Figure 5 shows the results of a numerical simulation performed with a laminar boundary layer of thickness  $\delta=10$  mm, a free stream velocity of 200 m/s, and a 2 mm thick aluminium skin covered with the ideal insulating dielectric layers described previously. The time sequence start at  $t=0$  s, it lasts 4 ms and each

frame is separated by 1 ms. It can be seen clearly that as the arc column is convected, its shape remains unchanged far from the skin. However, the arc shows a complex and dynamic evolution in the vicinity of the skin with the formation of loops of current close to the surface. This behaviour seems very chaotic but it is remarkable that the loops of current tend to exhibit quasi-periodic fluctuations when they are generated close to the hole (see figure 6). It results from the MHD instability described in figure 2, and the interaction with the flow and the solid skin. After some distance of propagation, far from the hole, the shape of the arc close to the skin becomes more chaotic. To be able to characterize in a more quantitative way the complex shape of DC arc columns, Tanaka has defined in [10] several influent parameters: The expansion radius, the normalized length, also called tortuosity (ratio of the arc column length to the gap length), and the internal voltage gradient. These parameters have proven to be well suited to characterize a DC arc column since Tanaka found that they are barely dependent on the geometry and that they depend only on the current value.

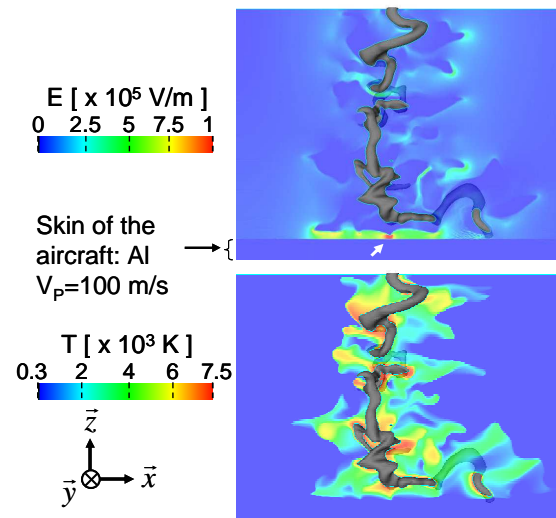


**Figure 4:** Numerical simulation of a swept arc on the aluminium skin of an aircraft flying at  $V_p=100$  m/s. The arc is visualized with the isosurface  $T=8000$  K just before a reattachment. The top picture shows a sliced view of the electric-field norm in the plane  $y=0$ . The bottom picture shows the corresponding temperature field. There is an important temperature gradient close to the maximum electric-field region where the next reattachment occurs.

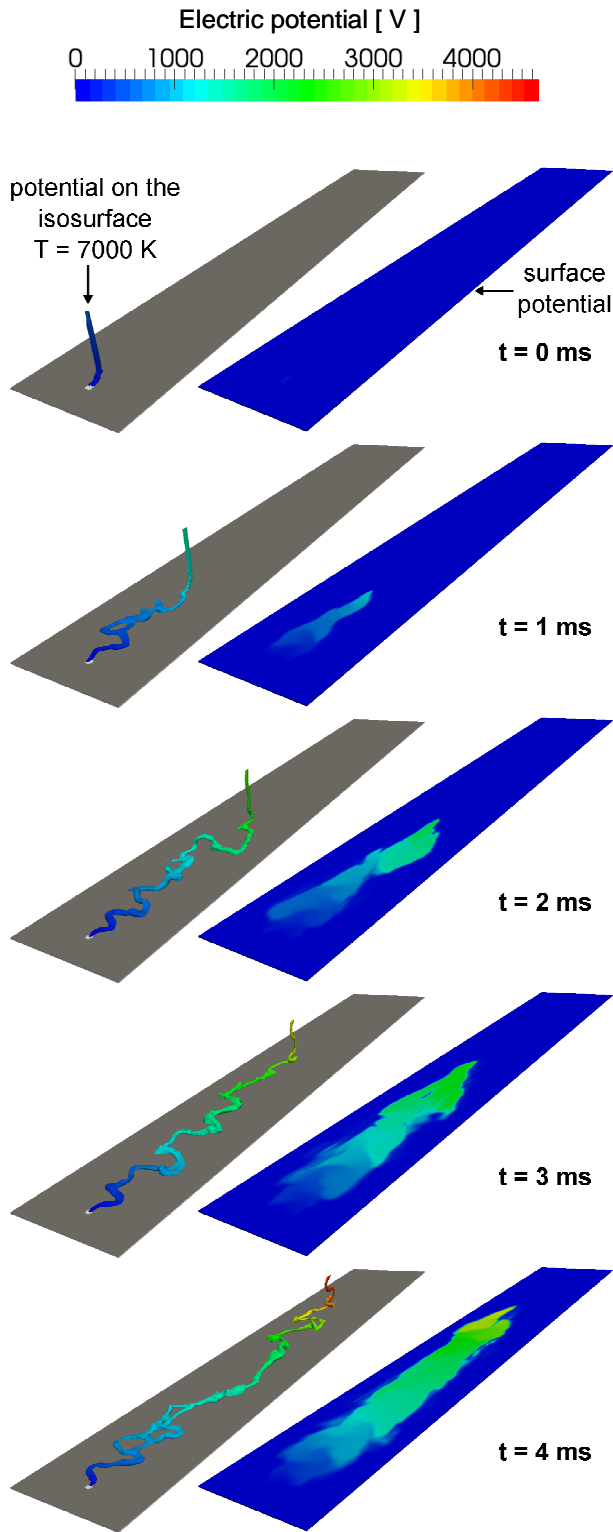


**Figure 5:** Evolution of a swept lightning arc on the skin of an aircraft. ( $I=400$  A,  $V_p=200$  m/s,  $\delta=10$  mm).

The expansion radius is defined as the distance from the center axis to the furthest point in the arc. In his work, Tanaka defined the center axis as the axis joining the electrodes. In our case, the center axis is defined on the skin surface (see figure 6), it is parallel to the free-stream flow and is joining the initial column position on the surface (the position of the hole). On figure 5, it can be seen that the expansion radius increases with time and finally stabilizes around an average value of about 7 cm. The limitation of the expansion radius is a consequence of the loop reconnection process explained on figure 2 and figure 6. Figure 6 shows clearly how the loop reconnection process is able to limit the spatial extension of the loops and the spreading of the arc on the skin. At  $t_5$ , several loops are formed at the same time and the current distribution is very tortuous. Because of this permanent loop creation and destruction, the normalized length of the arc is fluctuating between 1.6 and 1.8 and seems to increase with time.

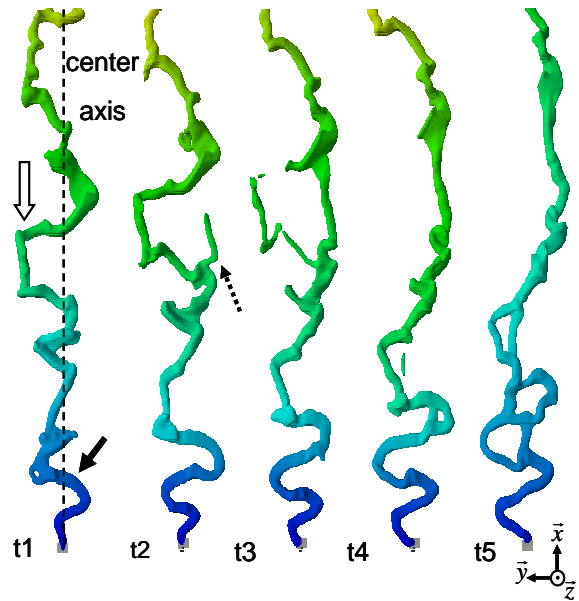


**Figure 6:** Loop reconnection process in the arc column, each frame is separated by  $50 \mu\text{s}$ .  $t_1$ : Loops are generated regularly close to the hole in the insulating layers (black arrow). Then they are convected by the flow and they grow under magnetic forces (white arrow) ;  $t_2$ - $t_3$ : when a loop is large enough a new arc is able to bridge the gap and close the loop (dashed arrow) ;  $t_4$ - $t_5$ : the arc becomes straight but new current loops and complex structures appear again near the hole.

These values of expansion radius and normalized length are close to the ones obtained by Tanaka [10] for the case of a 100 A DC arc column. For a DC arc column of 400 A, we should expect a larger expansion radius of about 15 cm and a normalized length around 1.8, but in our case the arc is stretch by the flow and moves mainly on the 2D surface of the skin. These two effects seem to decrease the expansion radius and the normalized length compared to the case of a free 3D DC column arc. Moreover, Tanaka has shown that the normalized length increases between 0 and 20 ms to finally form a plateau for larger timescales (figure 3 in [10]). It is then reasonable to assume that the presented simulations of 4 ms describe an arc during this transient phase of increasing tortuosity. Figure 7 shows a simulation performed with the same set of parameters as in figure 5 but with a two times thinner boundary layer of  $\delta=5$  mm. The arc structure is different than in the case of figure 5, which demonstrates the importance of the interaction between the aerodynamic flow in the boundary layer and the physics of the swept arc. However, interesting is to note that the normalized length, and expansion radius remain quite similar.

### Internal voltage gradient and reattachment

The internal voltage gradient, defined as the total potential difference divided by the length of the arc is very important for the swept stroke problematic. Under the assumption that the electric-field is homogeneous inside the arc column, it provides a good estimation of the electric-field encountered inside the column. In [10], Tanaka found that the internal potential gradient decreases with time between 1 kV/m initially to 0.7 kV/m at 100 ms for a free DC arc with a current of 100 A. The values obtained in the simulations of figure 5 and 7 give higher values, around 3 kV/m, but the presence of fluctuations make it difficult to observe a significant decrease with time during the first 4 ms. Moreover, the electric-field distribution in the arc column appears to be inhomogeneous. Figure 8 shows the distribution of the electric-field in the arc column on the isosurface  $T=7000$  K for the case with  $\delta=5$  mm (Figure 7). It appears that the electric-field presents some minimum outward the loops around 1 kV/m and conversely, it is maximum inward the loops where it can reach up to 10 kV/m.

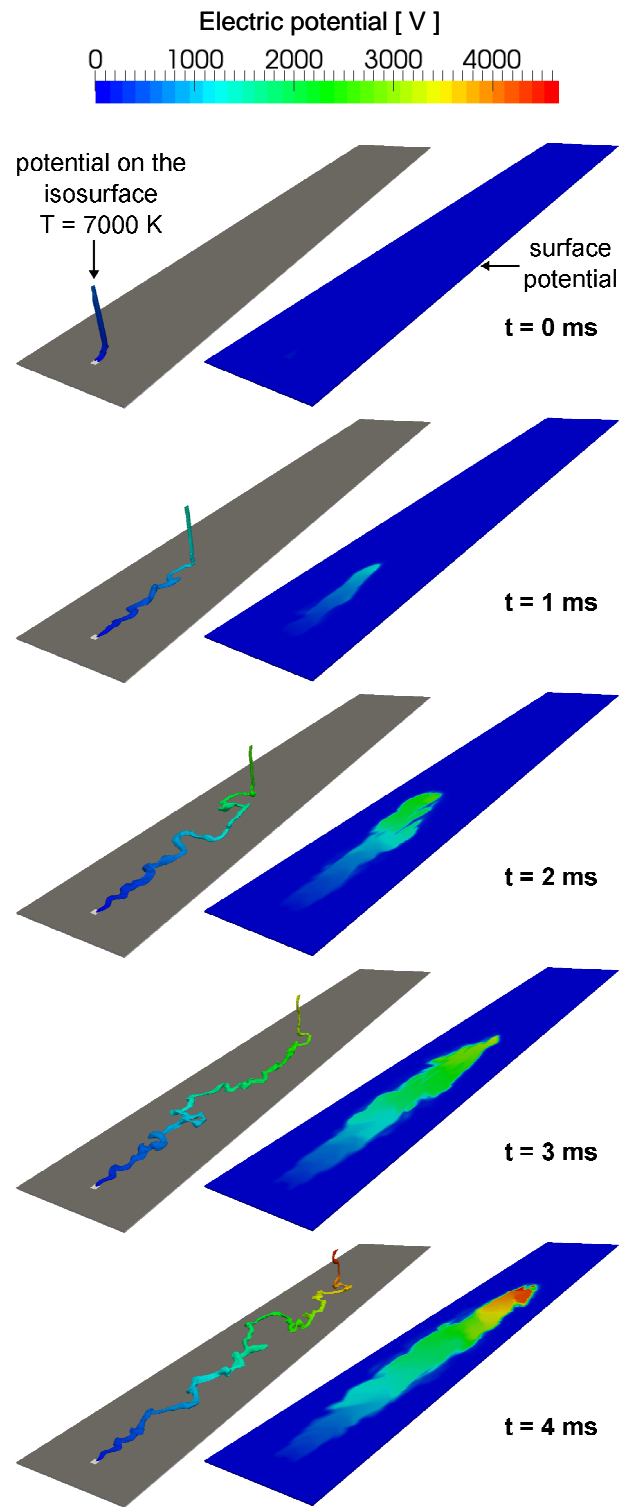


**Figure 7:** Evolution of a lightning arc during the sweeping of the skin of an aircraft. ( $I=400$  A,  $V_p=200$  m/s,  $\delta=5$  mm).

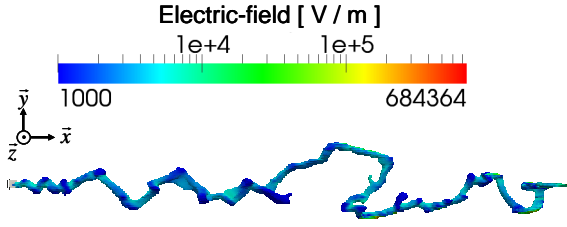


**Figure 8:** Electric-field distribution on the isosurface  $T=7000$  K for a swept lightning with  $I=400$  A,  $V_p=200$  m/s and  $\delta=5$  mm at  $t=4$  ms.

In [11], Larsson et al. have considered internal potential gradient values of 1 kV/m for the continuing current phase of a swept stroke. They conclude that the breakdown of the air gap between the lightning channel and the surface of the aircraft ( $\Delta x$  on figure 1) is very unlikely with such small electric-field values, and that the reattachment process is more likely during a restrike. For this purpose, they express a condition for the reattachment process of a lightning stroke as follow:

$$(2) \quad \varphi_p > E_B \cdot \Delta x + E_{B_{diel}} \cdot e_{diel}$$

According to this criterion, a reattachment is likely to occur if the potential  $\varphi_p$  in the plasma column is high enough to break through the air gap, of thickness  $\Delta x$  and dielectric strength  $E_B$ , between the arc and the plane, and through the insulating dielectric layer (paint layer), of thickness  $e_{diel}$  and dielectric strength  $E_{B_{diel}}$ . This model is directly related to the usual representation of the jump of the attachment point during a swept-stroke phenomenon represented in figure 1. However, figures 5 and 7 bring to light that the arc is really stuck to the surface from start to end. A better representation of a swept-stroke would then be the one represented schematically on figure 9: With this configuration, no air gap “ $\Delta x$ ” is present to insulate the dielectric layers from the plasma column and the plasma potential  $\varphi_p$  is applied directly on the top of the dielectric while the underneath conductive aluminium skin is almost grounded due to its high conductivity. Then the maximum surface potential is located directly under the arc column as it can be seen on figures 5 and 7. As a consequence, a simplest criterion for breakdown and reattachment can be written (equation 3):

$$(3) \quad \varphi_p > E_{B_{diel}} \cdot e_{diel}$$

The evolution of the potential  $\varphi_p$  with time can be obtained as a function of the arc properties and the velocity of the aircraft (equation 4):

$$(4) \quad \varphi_p = \varphi_0 + V_p \cdot NL_{arc} \cdot E_{arc} \cdot t$$

Where  $\varphi_0$  is the potential in the plasma column at the location of impact,  $V_p$  the velocity of the plane,  $NL_{arc}$  is the normalized length,  $E_{arc}$  the internal potential gradient and  $t$  the time. Then, a formula may be written for the dwell time  $\tau$  (equation 5).

$$(5) \quad \tau = \frac{E_{B_{diel}} \cdot e_{diel} - \varphi_0}{V_p \cdot NL_{arc} \cdot E_{arc}}$$

As expected, it shows clearly that the conditions promoting large dwell times correspond to small plane velocities, small tortuosity and internal potential gradients, and highly insulating layers (high dielectric strength and large thickness).

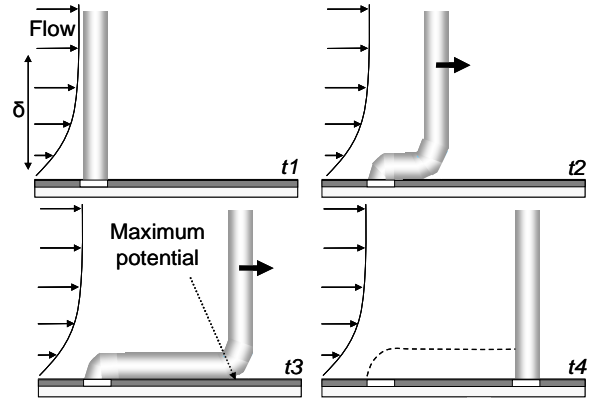


**Figure 9:** Schematic representation of a swept stroke on a flat surface. In this particular case, the arc column is stuck to the surface. The maximum surface potential is under the arc column.

Figure 10 shows the evolution as of the maximum surface potential over time for the numerical simulation with  $\delta=5$ mm (figure 7). This maximum is always located right under the arc column (see surface potential on figures 5 and figure 7). Due to the high tortuosity of the arc, the surface potential increase is faster than for the ideal case of a straight arc (normalized length  $NL=1$ ).

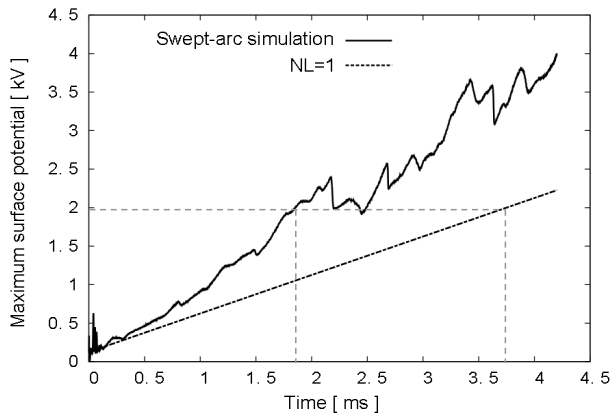


**Figure 10:** Evolution of the maximum surface potential for the swept arc simulation with  $\delta=5$  mm. Comparison with an ideal straight arc with no tortuosity ( $NL=1$ ).

The ratio between the two slopes is around 1.7, which is the averaged tortuosity for the simulated swept arc. The simulated case is then more favorable to the breakdown of the insulating layers. Consequently, the dwell-time is in this case smaller than for the case of a straight arc. For example, considering a paint layer of thickness  $200 \mu\text{m}$ , and a dielectric strength of  $10 \text{ kV/mm}$ , the surface potential necessary to produce the breakdown of the paint is  $2 \text{ kV}$ . According to figure 10, the corresponding dwell-time is  $3.7 \text{ ms}$  when considering a straight arc, and around  $1.8 \text{ ms}$  for the more realistic simulated arc. The straight arc case is then a majoring case for the estimation of the dwell time and the thermal constraints it could generate. We have shown that the boundary layer thickness has a very small influence on the normalized length and Tanaka's work demonstrates that it only depends on the electric current, with values ranging from 1.6 for DC arcs at  $100 \text{ A}$  to 2.1 for  $2000 \text{ A}$  [10]. Considering a swept arc tortuosity of 1.6 for example, would be a reasonable majoring estimation of the dwell-time, less constraining than the straight arc model. To be able to evaluate the dwell-times for highly insulating layers, such as polyethylene, with dielectric strength up to  $500 \text{ kV/mm}$  [12], it is possible to extrapolate the results of figure 10. Such extrapolation is reasonable since the tortuosity is expected to stabilize around a constant value after some time. Then, even if the normalized length increases slightly, the extrapolation would still give an accurate majoring value for the dwell-time. For a polyethylene layer of  $200 \mu\text{m}$  thickness, the dwell-time would then be

of the order  $100 \text{ ms}$ , which seems much larger than the typical value of dwell-time given in [1] for aluminum covered with paint ( $20 \text{ ms}$ ). The physical reason is probably the fast decrease of dielectric strength with temperature for organic compounds such as polyethylene. Figure 11 Shows a sliced view of the temperature profile inside the insulating layer in contact with the hot air plasma at  $t=4 \text{ ms}$  for the case with  $\delta=5 \text{ mm}$  (figure 7). The corresponding surface potential is also represented. The maximum temperature is around  $1300 \text{ K}$  close to the hole, but in most of the area in contact with the arc it is around  $500 \text{ K}$ . At the location of maximum potential, the temperature is less important and around  $400 \text{ K}$ . According to [12], at  $400 \text{ K}$ , the dielectric strength of polyethylene is divided by 5 compared to the value at  $300 \text{ K}$  ( $100 \text{ kV/mm}$  instead of  $500 \text{ kV/mm}$ ), and it seems to stabilize up to the pyrolysis temperature. A five time smaller dwell-time of  $20 \text{ ms}$ , equal to the value obtained in [1] is then to be expected when we take into account the combined electrical and thermal constraints. This underline the importance in future works to model properly the materials under transient and combined thermal and electrical constraints and very fast heating rates. Such data are very hard to find in the literature and would need more emphasis. Aside from this limitation, a careful attention should be paid to the fact that our numerical simulations consider a very ideal case with a planar skin, parallel to the free-stream flow, with a perfectly laminar boundary layer following the Blasius equation (no recirculation, no pressure gradients). To be more representative of a swept stroke during a landing or a take off phase, realistic shapes and the angle of attack should be taken into account because recirculation and boundary layer separations may increase the distance between the arc column and the skin and lead to a situation very different from figure 9. Further work is then necessary to perform similar simulations in a more realistic flow-field and geometry.

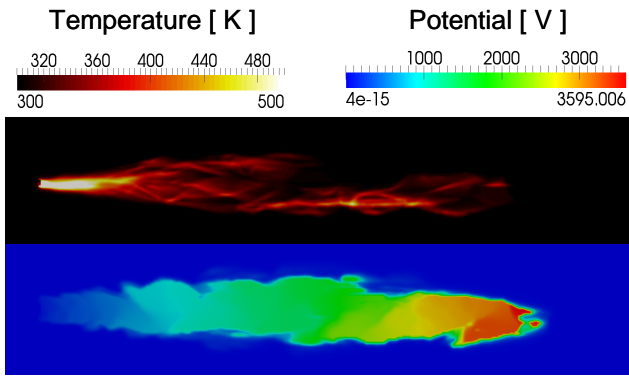


**Figure 11:** Distribution of the surface temperature (up) and the surface potential (down) for the swept arc simulation with  $\delta=5$  mm (figure 8) at  $t=4$  ms.

## Conclusion

The 3D MHD numerical simulations performed in this work allow us to determine the typical parameters a continuous swept-arcs with  $I=400$  A during 4 ms. In our particular conditions of velocity ( $V_p=200$  m/s) and boundary layer thickness ( $\delta=5$ -10 mm), the normalized length is found to be very close to the values obtained by Tanaka [11] for DC arc columns of smaller intensity ( $I=100$  A). The expansion radius is around 7 cm and the potential drop is around 3 kV/cm. However, non-uniform electric-fields are observed in the plasma channel due to the high tortuosity of the arc. The dynamics also reveals a continuous creation of loops of current close to the hole in the insulating layers that are generated at an almost constant frequency. These loops are MHD instabilities growing in size as they are convected by the flow that finally close themselves and extinguish when they reach a critical size. This reconnection process limits the spatial extension of the arc and induces large fluctuations of the expansion radius and the normalized length. The shape of the arc column appears to be different from the usual representation of swept stroke reattachment phenomenon: the arc is stuck to the surface, and no air gap is observed between the surface and the arc column. As a consequence, the maximum voltage is on the surface right under the arc column. The maximum surface-potential, is a key parameter that can be used to predict the breakdown of the insulating layers and the dwell time in our simplified geometry, but special attention should be paid to the breakdown

properties of materials under combined thermal and electrical constraints. However, the numerical model used in this work is well adapted to study in a next step more realistic geometries, flow configurations and material properties, especially for fuel tank areas.

## REFERENCES

- [1] Fischer F. A., Plumer J. A., and Perala R. A., *Lightning protection of aircraft*. NASA Reference Publication 1008, 1977.
- [2] Lalande P., Chemartin L., Peyrou B., "Magneto hydrodynamic modeling of the lightning arc channel in interaction with aircraft », Proceedings of the International Conference on Lightning and Static Electricity, United Kingdom, (2011)
- [3] Garren D. A. and Chen J., "Lorentz self-forces on curved current loops", *Phys. Plasmas* 1, 3425 (1994)
- [4] Chemartin L., Lalande P., Delalondre C., Cheron B., and Lago F., "Modelling and simulation of unsteady dc electric arcs and their interactions with electrodes," *J. Phys. D: Appl. Phys.*, vol. 44, no. 19, p. 194003, May 2011.
- [5] Swierczynski B., J. J. Gonzalez, P. Teulet, P. Freton, and A. Gleizes, "Advances in low-voltage circuit breaker modelling," *J. Phys. D: Appl. Phys.*, vol. 37, no. 4, pp. 595–609, Feb. 2004.
- [6] D'Angola A., G. Colonna, C. Gorse, and M. Capitelli, "Thermodynamic and transport properties in equilibrium air plasmas in a wide pressure and temperature range," *The European Physical Journal D*, vol. 46, no. 1, p. 22, 2008.
- [7] Archambeau F, Mechtoua N, Sakiz M, "Code\_Saturne: a finite volume code for the computation of turbulent incompressible flows, Industrial Applications", *International Journal on Finite Volumes*, Vol. 1, (2004).
- [8] Chemartin L., Lalande P., "simulation of a swept stroke discharge during lightning strike to aircraft with a three-dimensional electric arc model.", *Gas Discharges and their app.*, Greifswald, (2010).
- [9] Lalande P., Bondiou-Clergerie A. and Laroche P., "Analysis of available in-flight measurements of

lightning strikes to aircraft", Int. Conf. On Lightning and Static Electricity, Toulouse, France (1999)

[10] Tanaka S., Sunabe K. and Goda Y., "Three Dimensional behaviour analysis of D.C. free arc column by image processing technique", Gas Discharges and their app., Glasgow, (2000).

[11] Larsson A., Bondiou-Clergerie A., Lalande P., Delannoy A. and Dupraz S., "New methodology for determining the extension of lightning swept stroke zones on airborne vehicules", SAE 2001 Transactions, Journal of Aerospace 2001.

[12] Péliou S., St-Inge H., Wertheimer M. R., "Dielectric Breakdown in Polyethylene at Elevated Temperatures", IEEE Transactions on Electrical Insulation, vol. EI-19, no. 3, June 1984

[13] Dobbing J. A., Hanson A. W., "A swept stroke experiment with rocket sled", Proceedings of the International Symposium on Electromagnetic Compatibility, Atlanta, June 1978